

EDP2-1

Neutron signal features of Nb-based kinetic inductance detector with ^{10}B convertor

*Yuya Miki¹, Hiroyuki Yamaguchi¹, Yuki Iizawa¹, Hiroaki Shishido^{1,2}, Kenji M Kojima^{3,4}, Kenichi Oikawa⁵, Masahide Harada⁵, Shigeyuki Miyajima^{2,6}, Mutsuo Hidaka⁷, Takayuki Oku⁵, Kazuhio Soyama⁵, Takekazu Ishida^{1,2}

Department of Physics and Electronics, Osaka Prefecture University, Sakai, Osaka 599-8531, Japan¹

NanoSquare Research Institute, Osaka Prefecture University, Sakai, Osaka 599-8531, Japan²

Muon Science Laboratory and Condensed Matter Research Center, Institute of Materials Structure Science, KEK, Tsukuba, Ibaraki 305-0801, Japan³

Department of Materials Structure Science, The Graduate University for Advanced Studies, Tsukuba, Ibaraki 305-0801, Japan⁴

Materials and Life Science Division, J-PARC Center, Japan Atomic Energy Agency, Tokai, Ibaraki 319-1195, Japan⁵

Advanced ICT Research Institute, NICT, Kobe, Hyogo 651-2492, Japan⁶

National Institute of Advanced Industrial Science and Technology (AIST), Tsukuba⁷

Our kinetic inductance neutron detector is made of a 40-nm-thick Nb meanderline and a ^{10}B conversion layer with the effective area of $15 \times 15 \text{ mm}^2$ on a single Si chip ($22 \times 22 \text{ mm}^2$), and is biased by a small DC current I_b at a temperature below T_c . A meanderline of the kinetic inductance detector exhibits a transient change occurs in the kinetic inductance $\Delta L_K = m_s \Delta l / n_s q^2 S$ of a mesoscopic portion (possible hot spot), where m_s is the effective mass of a Cooper pair, q_s is the effective electric charge, n_s is the Cooper pair density, Δl is the length of the hot spot, and S is the cross-sectional area of the Nb wire. We expect that the voltage V is proportional to a product of the bias current I_b and a time derivative of the kinetic inductance $d\Delta L_K/dt$, and a pair of signals propagate along the Nb stripline as an electromagnetic wave at a certain fraction of the light velocity c toward electrodes. We conducted the neutron irradiation experiment at J-PARC. The nuclear reaction $^{10}\text{B}(n, ^4\text{He})^7\text{Li}$ releases a ^4He particle of 1.47 MeV and a ^7Li particle of 0.88 MeV, and the energy of each projectile is used to create a hot spot on the Nb nanowire of the detector. It remains to be answered why the signal voltage shows such a continuum in the histogram of the signal height even if the incident energy of the light ion is apparently monochromatic. We also investigated the distribution of the width of the signal pulse. The height and width of the signal has a clear correlation, which might be is the key of understanding the operating principle of our detector. We consider that the origin of the signal distribution is due to the positional dependence of the light ion bombardment with respect to the meandering Nb nanowire.

This work is supported by Grant-in-Aid for Scientific Research (S) No. 23226019, Grant-in-Aid (A) No.16H02450 from JSPS. The devices were fabricated in the clean room for analog-digital superconductivity (CRAVITY). This work is partially benefitted by the use of (VDEC, the University of Tokyo with the collaboration with Cadence Corporation. This work is supported of MLD program (Proposal No. 2015A0129, No. 2015P0301).

Keywords: Kinetic inductance detector , Operation principle, Neutron , Signal profile

EDP2-2

Electrodynamic Theory for the Operation Principle of Superconducting Delay-line Kinetic Inductance Detector

*Tomio Koyama¹, Takekazu Ishida^{1,2}

Department of Physics and Electronics, Osaka Prefecture University¹
Institute for Nano-Fabrication Research, Osaka Prefecture University²

Generation and propagation of voltage signals in a superconducting delay-line inductance detector, which has been developed for a high-performance radiation detector, is theoretically investigated in terms of superconducting electrodynamics. The detector consists of a meandering superconducting nanowire deposited on a substrate composed of a stack of insulating and superconducting layers. It is shown that this system can be regarded as a superconducting waveguide. We derive a dynamical equation for the superconducting phase difference between the superconducting nanowire and the substrate superconducting layer. This equation predicts the generation of a pair of voltage pulses with opposite polarities when a transient hot spot appears inside the current-biased nanowire. The pair of voltage pulses splits into two single pulses propagating in the opposite directions to each other. The velocity of the voltage pulses along the delay-line is well fitted by our theory.

Keywords: kinetic inductance detector, superconducting nanowire, superconducting theory

EDP2-3

Signal propagation in delay-line kinetic inductance detector under DC bias current

*Yuki Iizawa¹, Hiroyuki Yamaguchi¹, Yuya Miki¹, Kazuma Nishimura¹, Hiroaki Shishido^{1,2}, Kenji M. Kojima³, Kenichi Oikawa⁴, Masahide Harada⁴, Shigeyuki Miyajima^{2,5}, Mutsuo Hidaka⁶, Takayuki Oku⁴, Kazuhiko Soyama⁴, Tomio Koyama⁷, Takekazu Ishida¹

Department of Physics and Electronics, Osaka Prefecture University, Sakai, Osaka 599-8531, Japan¹

NanoSquare Research Institute, Osaka Prefecture University, Sakai, Osaka 599-8531, Japan²

Muon Science Laboratory and Condensed Matter Research Center, Institute of Materials

Structure Science, KEK, Tsukuba, Ibaraki 305-0801, Japan³

Materials and Life Science Division, J-PARC Center, Japan Atomic Energy Agency, Tokai, Ibaraki 319-1195, Japan⁴

Advanced ICT Research Institute, NICT, Kobe, Hyogo 651-2492, Japan⁵

National Institute of Advanced Industrial Science and Technology (AIST), Tsukuba, Japan⁶

Institute for Materials Research, Tohoku University, Sendai, Miyagi 980-8577, Japan⁷

We developed a high resolution imaging system by using a current biased kinetic inductance detector (CB-KID) operating in a delay-line mode. It consists of stacking layers of a superconducting Nb ground plane, SiO₂ insulator, and a two set of superconducting Nb meanderlines. When some amount of energy is deposited to the superconducting wire of the meanderline, it produces a hot spot in a tiny segment of the wire, where Cooper pairs are suppressed locally, and induces a temporal change of the kinetic inductance there. If a DC-bias current flows along the meanderline, the transient change in the kinetic inductance excites voltage pulses, which propagate toward both ends of the Nb stripline with opposite polarities. We observe the arrival signals by a digital oscilloscope to store the wave forms. We use the arrival timestamps to identify the hot-spot position of the wire by knowing a time difference in arrival timestamps and the propagation velocity. This is the method how we image the distribution of mesoscopic excitations in both X and Y detectors by irradiation of pulsed neutrons. Therefore, it is important to investigate the propagation velocity before conducting imaging experiments. We applied a test pulse from one end of meander, and the transmitted signal was measured at another end to know the velocity. The basic equation for signal propagation has been derived by Koyama *et al.* by using the Maxwell-London theory on a superconducting waveguide of nanowire - SiO₂ - ground plane (S-I-S) structure. In the theory, the electromagnetic wave is treated as a Swihart pulse. As shown in Fig. 1, we successfully fit the propagation velocity as a function of temperature by using the equation shown in the figure. Since the superfluid density decreases as the temperature increases, the velocity comes from a change in the kinetic inductance. We plan to investigate the velocity as a function of DC bias current, too. The systematic comparison between theory and experiment would be interesting.

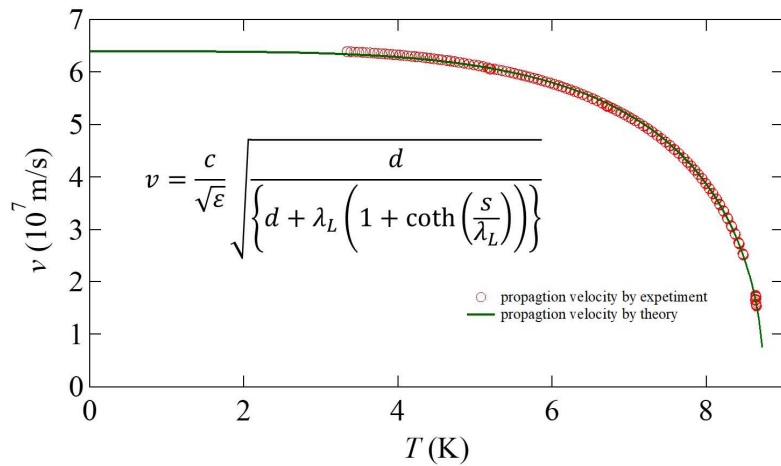


Fig. 1. The propagation velocity in the CB-KID as a function of temperature. Solid line is a fit by the Maxwell-London theory.

Keywords: Kinetic inductance detector, Propagation velocity, Maxwell-London theory

EDP2-4

1 dimensional X-ray imager utilizing a superconducting strip line with a delay line structure

*Chiharu Watanabe¹, Nobuyuki Zen¹, Go Fujii¹, Kazumasa Makise¹, Masahiro Ukibe¹, Masataka Ohkubo¹

AIST, Nanoelectronics Research Institute¹

Now days, Resonant Inelastic soft X-ray Scattering (RIXS) technique have been eagerly developed to study the electrical state of transition metal oxide which shows interesting character such as high- T_c superconductivity and giant magneto resistive effect. In addition, since RIXS utilizes resonant excitation of electrons, it is expected to analysis electrical state with higher resolution because of the larger signal amplitude.

Generally, the luminescence X-ray spectra are detected by the combination of a grating and an image detector such as a CCD camera in order to measure them with higher energy resolution than by ordinal wavelength dispersion type X-ray spectrometers based on semiconductors. However, sufficient spatial resolution (<1 mm), for analysis of such as high- T_c superconductors, can not be obtained by X-ray CCD detectors based on semiconductors. On the other hand, sub mm spatial resolution of 1D-photon imaging was obtained by the combination of the superconducting strip photon detector (SSPD) and the delay line structure [1].

Therefore, we tried to develop 1D-delay line photo imager utilizing SSPD which has 0.5 mm spatial resolution and large active area (> 5 x 10 mm²). In order to validate if such a structure can work, we calculated the distributed circuit consisting of 10,000 segments of LC which explain a superconducting strip line (width: 400 nm, length: 1 m). As a result, since we obtained the sharp signal rise time which is less than 1 nsec, we found that it is expected to get sufficient spatial resolution for RIXS.

Reference [1] Qing-Yuan Zhao *et al.*, Nat. Photon. **27**, 247 (2017).

Keywords: Superconducting Strip Photon Detector, X-ray detector, RIXS

EDP2-5

Study for the Operating Principle of Superconducting Strip Photon Detectors (SSPDs)

*Nobuyuki Zen¹, Yutaka Abe², Go Fujii¹, Yuma Tomitsuka², Yuki Yamanashi², Yasunori Mawatari¹, Nobuyuki Yoshikawa²

National Institute of Advanced Industrial Science and Technology, JAPAN¹

Yokohama National University, JAPAN²

Superconducting strip photon detectors (SSPDs) are promising single photon detectors for realizing practical quantum cryptography; their high quantum efficiencies, low timing jitters, and low dark count rates overcome those of avalanche photo diodes or other single photon detectors. Recently, some research groups have established testbeds for quantum cryptography and succeeded in field tests of quantum key distribution at a speed of sub Mbps using practical optical fibers in the length of tens of km.

However, the detecting mechanism of the SSPD is still under investigation. The most probable hypothesis is the followings: (1) an incident photon fluctuates the order parameter of a superconducting strip resulting in the nucleation of vortex-antivortex pairs; (2) vortex pairs are unbound and forced out of the strip in the perpendicular direction of bias current; (3) kinetics of vortices forms a normal band across the strip and a current pulse flows out of the strip. Conventional SSPDs utilize the current pulse as a photon detection signal and its response characteristics such as a response time of several ns regulate the quantum communication speed of sub Mbps as mentioned above.

On the other hand, the numerical simulations have shown that the time scale of kinetics of vortices is in the range of ps. Therefore, by detecting the extruded vortices instead of current pulse, we could expect the communication speed faster than several orders of magnitude of that realized by conventional SSPDs. In this study, we have directly connected a superconducting strip with single flux quantum (SFQ) circuits to capture the extruded vortices out of the strip. Since the information carriers of SFQ circuits are also vortices, not only capturing the vortices but also counting the number of the vortices or other logical operations are possible.

Keywords: SSPD, SFQ

EDP2-6

HTS Filter with Dielectric Rods For Tuning the Center Frequency and Trimming the Passband Characteristics

*Takahiro Unno¹, Naoto Sekiya¹

University of Yamanashi¹

Tunable filters are one of the most essential microwave components for multiband communication systems due to their attractive features. In this study, we developed high-temperature superconducting (HTS) tunable microstrip line filter with dielectric rods for tuning the center frequency and trimming the passband characteristics simultaneously. Several dielectric rods are placed above the HTS filter, and the center frequency and passband characteristics are controlled by changing the distance between the dielectric rods and resonators. Two dielectric rods are used for a resonator; one is located on the center of the resonator to tune the center frequency and trim the passband characteristics, and the other is located on the open end of the resonator to tune the center frequency. The filter was designed to have a center frequency of 1.4 GHz and a bandwidth of 28 MHz by using an electromagnetic simulator based on the moment method. The HTS filter was fabricated using double-sided $\text{YBa}_2\text{Cu}_3\text{O}_7$ thin film on a $30 \times 40 \times 0.5$ mm Al_2O_3 substrate. The dielectric rods with a dielectric constant of 40 were used. Figure 1 shows frequency responses of the tunable filter as a function of distance between the resonator and dielectric rods. The tuning range of the filter was about 140 MHz while keeping the all most the same insertion loss with trimming. The measurement data after trimming and tuning have a good agreement with the design specifications.

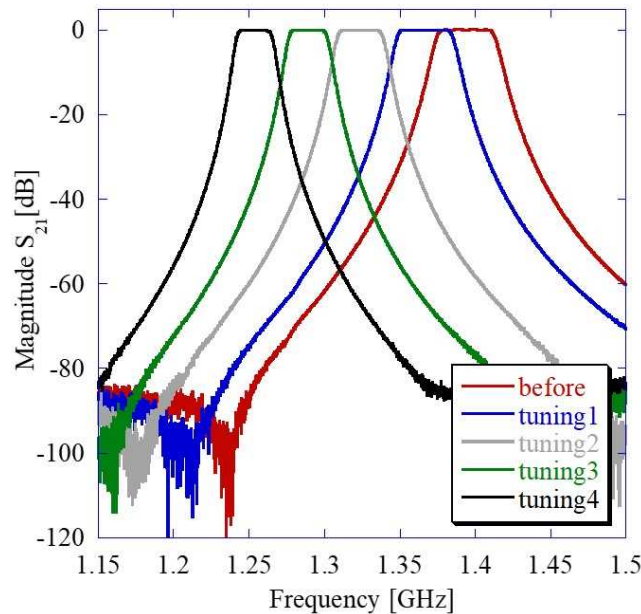


Figure 1 Measured tunability of 4-pole tunable filter before and after tuning.

Keywords: High-temperature superconducting (HTS), tunable bandpass filter,, dielectric rods, microstrip filter

EDP2-7

Design of wireless power transfer system from HTS spiral coil to copper spiral coil

*Shinya Kobayashi¹, Naoto Sekiya¹

University of Yamanashi¹

We have designed a wireless power transfer (WPT) system with high temperature superconducting (HTS) transmit coil and copper receiving coil. The WPT system was designed with bandpass filter theory. The WPT system is consisted of HTS spiral coil, copper spiral coil and two input and output loop coils. The HTS spiral coil was used a double-side HTS tape wire which we proposed before [1]. The center frequency of the WPT system is about 10 MHz. Vector network analyzer was used to measure the frequency response of the WPT system. To design the WPT system, we measured coupling coefficient between spiral coils and external coupling between spiral coil and loop coil. The measured quality factor of the HTS and copper coils are 3200 and 980, respectively. Figure 1(a) and (b) show the measured frequency responses of the WPT system with HTS transmit coil and copper coil and with two copper coils in 50-cm distance between two coils. Good frequency responses were obtained. The transfer efficiency of the WPT systems calculated from Fig. 1(a) and (b) is 73.6 and 61.5 %, respectively.

[1] N. Sekiya, Y. Monjugawa, "A novel REBCO wire structure that improves coil quality factor in MHz range and its effect on wireless power transfer systems," *IEEE Trans. Appl. Supercond.* vol. 27, 6602005, 2017-6.

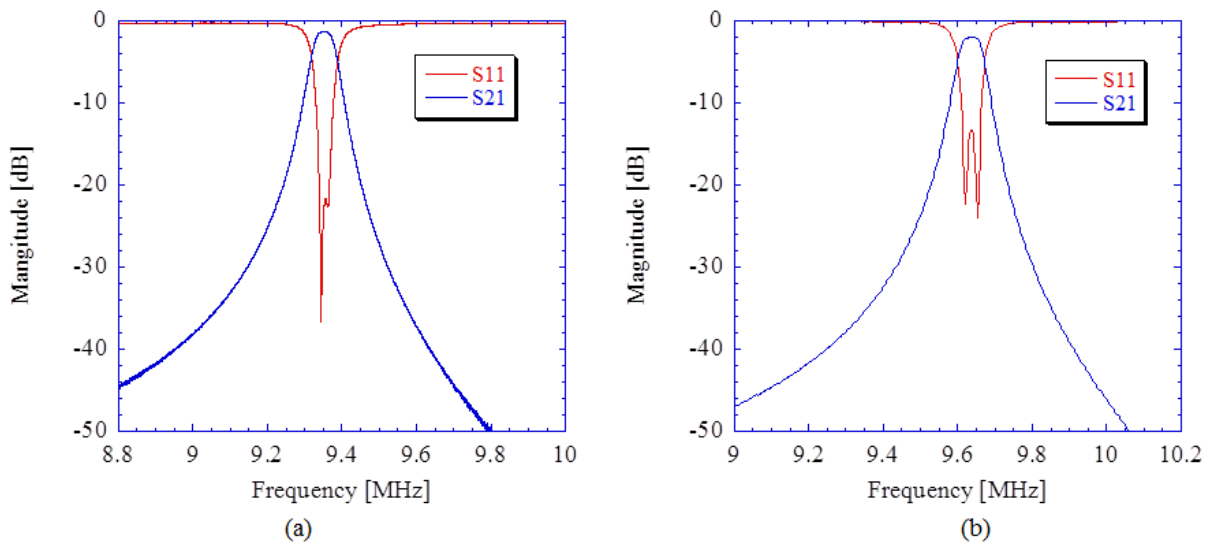


Fig. 1. Measured results of frequency responses in 50-cm distance. (a) HTS transmit coil and copper receiving coil. (b) Two copper coils.

Keywords: wireless power transfer, high temperature superconducting, spiral coil

EDP2-8

Pico Pulse Response Analysis of High-Tc Josephson Weak-Link using Time Dependent Ginzburg-Landau Model

*Shigeru Yoshimori¹

Faculty of Engineering, Takushoku University, 815-1 Tatemachi, Hachiojishi, Tokyo 193-0985 Japan¹

In this paper, we report on the pico pulse response analysis of high Tc superconducting Josephson weak-link in the terahertz region. We assumed Bi₂Sr₂Ca₂Cu₃O₁₀ as high Tc superconducting material. Tc and coherence length of Bi₂Sr₂Ca₂Cu₃O₁₀ are 110[K] and 1[nm], respectively. Terahertz wave is the electro-magnetic wave whose frequency is ranging from 0.1 to 10 THz and is going to be useful for high speed and high capacity telecommunicating, imaging, biological and chemical analyzing.

Since the photon energy of terahertz radiation is greater than the energy gap of high Tc superconductor, we used the one dimensional time-dependent Ginzburg-Landau (TDGL) equation. For example, pico pulse signal of 0.5[ps] wide consists of harmonic component greater than 10[THz]

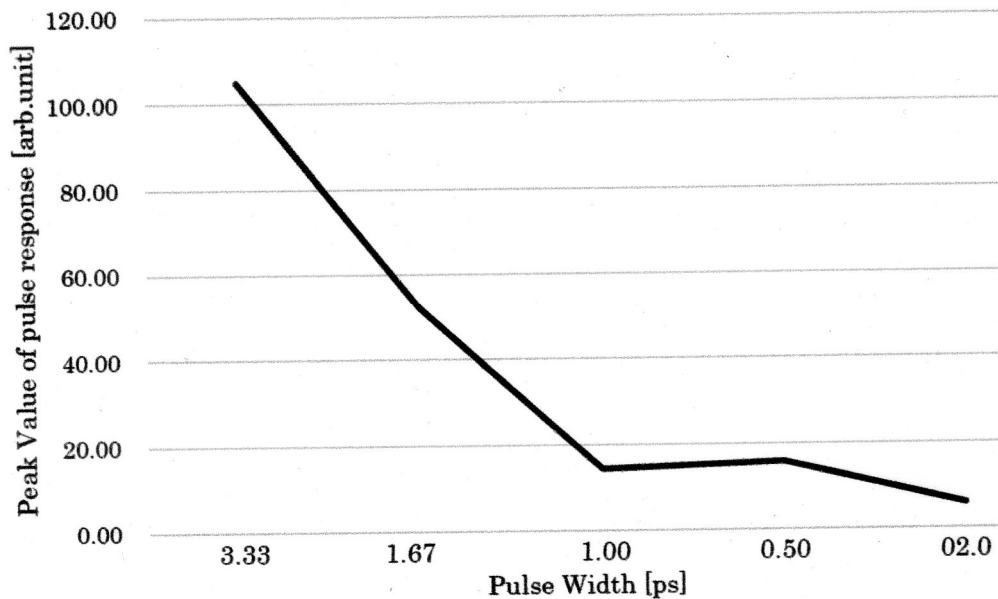
We derived the TDGL model as the equivalent circuit of Josephson weak-link by use of the TDGL equation, instead of the RSJ model [1]. In our analysis, R_n, normal resistance of the Josephson weak-link at T>T_c is assumed to be 1[Ω] and pulse response is normalized by the I_cR_n product where I_c is the critical current of the Josephson weak-link. Following results were found.

The normal resistance of the Josephson weak-link at T<T_c is not constant but dependent on the applied voltage.

The cosine φ term with negative sign appears in the TDGL model.

We analyzed pico pulse response at 50[K] and found that peak of pulse response decreased when the pulse width became short as shown in Fig.1.

[1] S. Yoshimori, T. Terashima and M. Kawamura, Infrared Physics & Technology, Vol.39, pp.41-45(1998).



Keywords: THz region, High-Tc Josephson weak-link, TDGL model, pico pulse response

EDP2-9

Microfabrication of MgB₂ by a conventional lift-off process

*Takatoshi Nakagami¹, Hiroaki Shishido^{1,2}, Takekazu Ishida^{1,2}

Department of Physics and Electronics, Japan¹
NanoSquare Research Institute, Japan²

MgB₂ is a superconductor with a remarkably high superconducting transition temperature $T_c = 39$ K [1] and an extremely short electron-phonon scattering time $\tau_{e-ph} \approx 3$ ps [2]. These characteristic features have impacts on not only basic research but also applied physics. However, a convenient microfabrication method applicable to MgB₂ has not been established yet because of the lack of a thin film growth process without heating up. Recently, we have succeeded in epitaxial growth of MgB₂ thin film with Mg buffer layer under a significantly low substrate temperature of 110 °C by using a molecular beam epitaxy (MBE) method [3]. The MgB₂ thin films thus obtained exhibits superconductivity with $T_c = 27$ K in spite of such low growing temperature. We demonstrate a microfabrication by a conventional lift-off process using an organic photoresist (Clariant AZ 5214 E) for MgB₂ thin films grown at low temperatures.

The Mg buffer layer of 24-nm thick was deposited with the deposition rate of 1.3×10^{-2} nm/min on a photoresist-patterned sapphire substrate by using the MBE method. After the Mg buffer layer deposition, the 96-nm thick MgB₂ layer was deposited under ultra-high vacuum of 3.3×10^{-7} Pa with the deposition rate of 3.8×10^{-2} nm/min by the co-evaporation of Mg and B, which were deposited by the Knudsen cells. The deposition rate ratio between Mg and B was the same as the exact stoichiometric ratio of Mg:B = 1:2. A 53-nm thick Bi layer was deposited on top of the MgB₂ film as a passivation layer. We successfully fabricated a 100- μ m stripline of MgB₂ by a conventional lift-off process and confirmed the superconductivity below 20 K.

[1] J. Nagamatsu *et al.*, Nature **410**, 63 (2001).

[2] B. B. Jin *et al.*, Supercond. Sci. Technol. **18**, L1 (2005).

[3] H. Shishido *et al.*, App. Phys. Express **8**, 113101 (2015), H. Shishido *et al.*, J. Phys.: Conf. Series **871**, 012036 (2017).

EDP2-10

Replacement of NbN by $\text{YBa}_2\text{Cu}_3\text{O}_{7-\delta}$ in Superconducting Thin Film Coil in a Spiral Trench on a Si-Wafer for Compact SMESs

*Yushi Ichiki¹, Kazuhiro Adachi², Yasuhiro Suzuki², Akihisa Ichiki², Tatsumi Hioki², Che-Wei Hsu³, Shinya Kumagai³, Minoru Sasaki³, Joo-Hyong Noh⁴, Osamu Takai⁴, Hideo Honma⁴, Tomoyoshi Motohiro^{1,2}

Graduate School of Engineering, Nagoya University, Furo-cho, Chikusa-ku, Nagoya, 464-8603, Japan¹
Green Mobility Research Institute, Institutes of Innovation for Future Society, Nagoya University, Furo-cho, Chikusa-ku, Nagoya, 464-8603, Japan²

Graduate School of Engineering, Toyota Technological Institute, Hisakata 2-12-1, Tempaku-ku, Nagoya 468-8511, Japan³

Materials & Surface Engineering Research Institute, Kanto-Gakuin University, 1162-2, Ogikubo, Odawara, Kanagawa 250-0042, Japan⁴

We have been developing superconducting thin film coils in a spiral trench on a Si wafers for compact SMESs as shown in Fig.(a). A proof of concept has been performed using NbN thin films showing energy storage of 0.01 mJ [1]. Increasing NbN thickness by mitigating film stress, the stored energy increased up to 0.1 mJ [2]. For further improvement, we moved on to replacement of NbN by $\text{YBa}_2\text{Cu}_3\text{O}_{7-\delta}$. Firstly, sputter-deposition of yttria stabilized zirconia succeeded by CeO_2 has been performed to form buffer layers to grow c-axis oriented $\text{YBa}_2\text{Cu}_3\text{O}_{7-\delta}$. By tuning the deposition conditions, (100) preferred orientations were attained in both layers. Deposition of $\text{YBa}_2\text{Cu}_3\text{O}_{7-\delta}$ was performed by metal organic deposition (MOD) using a commercially available raw material for MOD: KOJUNDO CHEMICAL LAB, YBC-05(1/2/3). The post deposition annealing (PDA) for 90 min in 1000 ppm O_2/N_2 was followed by annealing at 500 °C for 100 min in pure O_2 . PDA at 830 °C resulted in formation of BaCeO_3 as shown in Fig.(b). By decreasing PDA temperature, c-axis oriented $\text{YBa}_2\text{Cu}_3\text{O}_{7-\delta}$ emerged while BaCeO_3 faded out. To enhance the c-axis orientation of the MOD film, sputter-deposition of $\text{YBa}_2\text{Cu}_3\text{O}_{7-\delta}$ prior to MOD was also examined. More detailed findings and points obtained for the replacement of NbN by $\text{YBa}_2\text{Cu}_3\text{O}_{7-\delta}$ are to be analysed.

This work is partly supported by NEDO (16101979-0)[1] N.Sugimoto et al.SUST30 (2017) 015014. [2] Y.Suzuki et al. Proc.ISS2016, JPCS871(2017) 012071.

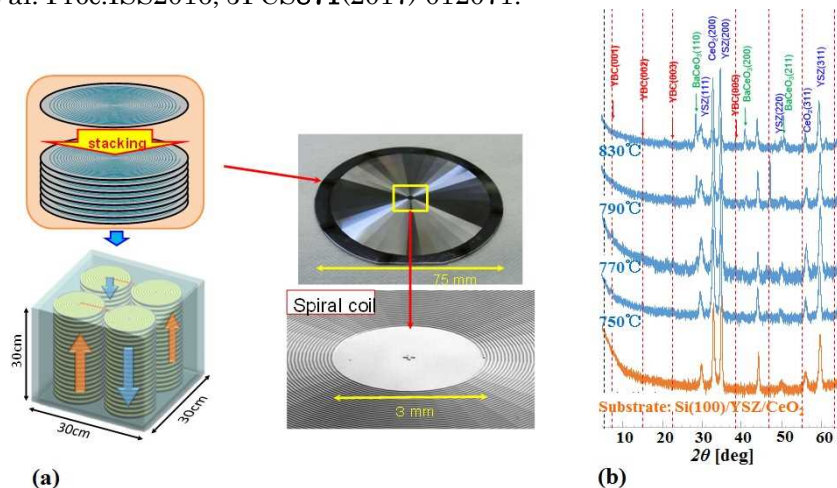


Fig.(a) Superconducting coil composed of 4 units. Each of the units is made of stacked Si wafers engraved with a superconducting thin film coil in a spiral trench formed with MEMS technology. (b) X-ray diffraction patterns of $\text{YBa}_2\text{Cu}_3\text{O}_{7-\delta}$ films on sputter-deposited CeO_2/YSZ thin film buffers at different post-deposition annealing temperatures

Keywords: SMES, Si wafer, NbN, $\text{YBa}_2\text{Cu}_3\text{O}_{7-\delta}$

Numerical Analysis of Rapid Single-Flux-Quantum Circuits Composed of 0- and π -Shifted Josephson Junctions

*Tomohiro Kamiya¹, Soya Taniguchi¹, Kyosuke Sano¹, Masamitsu Tanaka¹, Akira Fujimaki¹

Department of Electronics, Nagoya University, Japan¹

We report numerical analysis of rapid single-flux-quantum (RSFQ) circuits using combination of 0- and π -shifted Josephson junctions. The π -shift in phase difference is observed in several types of Josephson junctions, for example, a sandwich structure of superconductor electrodes and a ferromagnetic thin layer. We use a dc-SQUID including 0- and π -shifted Josephson junctions as a basic element, where bistability is obtained by the persistent current in either the counterclockwise or clockwise direction. This can lead to the following features: (1) reduction in power consumption with less bias points, (2) efficient circuit designs with a fewer number of junctions, and (3) smaller circuit areas because of eliminating large-inductance superconductor loops to store magnetic flux quanta, which are required in conventional RSFQ circuits to represent binary information.

We obtained successful operation of a toggle flip-flop (TFF) that was composed of two Josephson junctions (J_0 , P_1) as shown in Fig. (a). The P_1 and P_2 are π -shifted junctions, while J_0 and J_3 are normal (0-shifted) junctions. The input signals provided from a dc-SQUID (P_2 , J_3) were divided to the two outputs as shown in Fig. (b). Our numerical simulation showed that the efficient TFF could be constructed with half the number of junctions with no bias current ports, and the bias currents to P_2 and J_3 could be reduced to approximately $2/3$, compared with the conventional RSFQ TFF and Josephson transmission line.

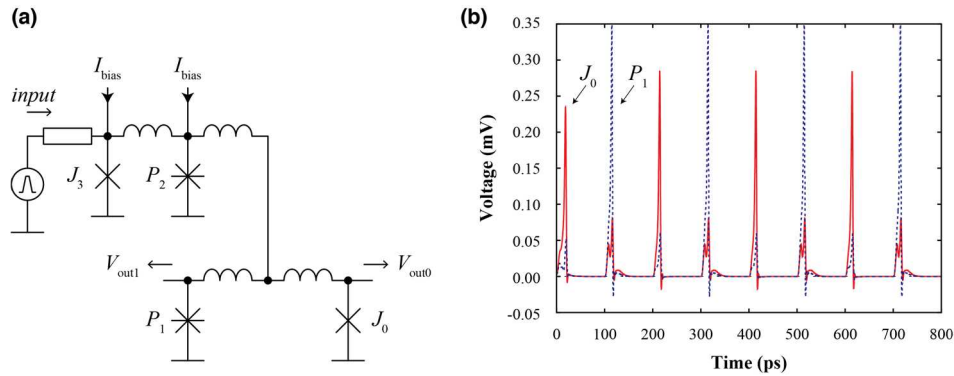


Fig. (a) equivalent circuit of a toggle flip-flop, (b) output signals. The inductance L , Josephson critical currents I_c , and bias currents I_{bias} are 2 pH, 200 μ A, and 90 μ A, respectively.

Acknowledgment: This work was supported by Grant-in-Aid for Scientific Research A (16H02340). The authors would like to thank Yuki Yamanashi for help in the numerical simulating.

Keywords: π Josephson junctions, rapid single-flux-quantum, low-power consumption, efficient circuit design

EDP2-12

High Impedance Josephson Junction Arrays for Voltage Standard Circuits.

*Hirotake Yamamori¹, Michitaka Maruyama², Yasutaka Amagai², Takeshi Shimazaki²

Nanoelectronics Research Institute, National Institute of Advanced Industrial Science and Technology¹

National Metrology Institute of Japan, National Institute of Advanced Industrial Science and Technology²

For voltage standard circuits, tens of thousands Josephson junctions connected in series consist of a co-planar waveguide, and microwaves or pulse codes are applied to them to generate the Shapiro step [1-2]. Both the larger output voltage (the number of junctions N) and the larger operating margin (the step height) are required. However, the large number of the junction N decreases the operating margin due to dissipation for applied microwaves in the junction, because microwave power P at N -th junction is given by $P = P_0 \exp(-N R_N/Z)$, where R_N is the junction resistance.

We designed the characteristic impedance of the array Z to be 100 Ω , while that for the conventional one was 50 Ω as shown in Fig.(a), because the high impedance array might contribute to increase the operating margin due to the smaller electric loss across the array. As shown in Fig.(b), the array including 19,199 Josephson junctions generated the flat voltage step at about 0.4 V, that suggested the array was working properly.

[1] S.P.Benz et al., IEEE Trans. on Appl. Supercond., Vol.25, p. 1300108 (2015).

[2] M.Maruyama et al., J. of Phys. Conf. Series, Vol.234, p.042020 (2010).

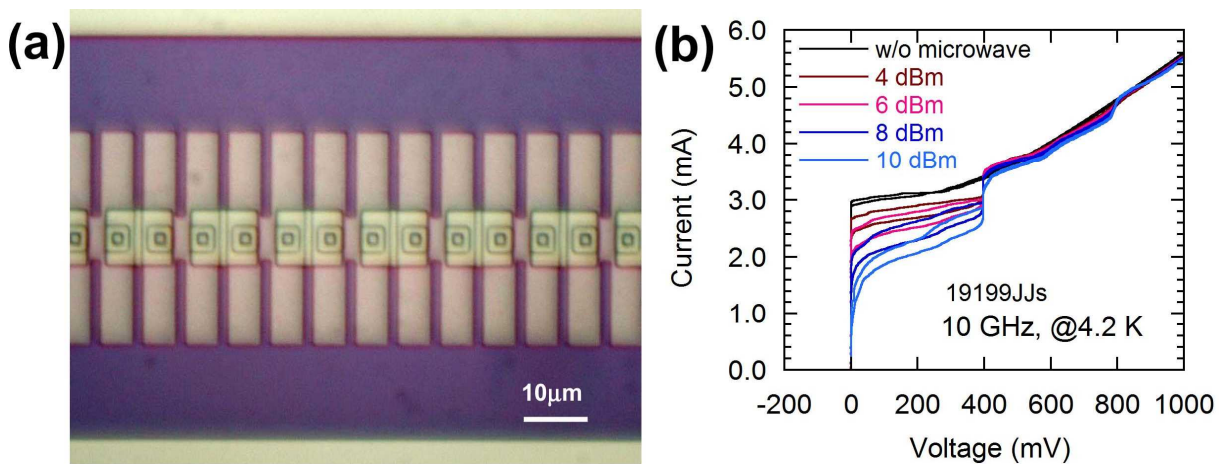


Fig. (a) Fabricated Josephson junction array, the junction size is 3 μm , (b) measured I - V characteristics for 19,199 NbN/TiN/NbN Josephson junctions with different microwave powers of 10 GHz at 4.2K.

The devices were fabricated in the clean room for analog-digital superconductivity (CRAVITY) in National Institute of Advanced Industrial Science and Technology (AIST). This work was partially supported by JSPS KAKENHI Grant No. 17K06481.

Keywords: Voltage Standard, NbN, CPW, Shapiro Step

EDP2-13

Negative resistance in niobium titanium nitride nanowires for flux-based superconducting devices

*Kazumasa Makise¹, Takayuki Asano³, Bunju Shinozaki², Masahiro Ukibe¹

National Institute of Advanced Industrial Science and Technology¹

Kyushu University²

University of Fukui³

Superconducting devices on nanowire have attracted much attention owing to easy fabrication. Because the nanowires do not use an insulating tunnel barrier, such as Josephson junction and their critical current is tuned by the wire diameter. We present temperature dependence of resistance and current-voltage characteristics of niobium titanium nitride (NbTiN) nanowire with different width and length. Firstly, superconducting NbTiN films were firstly prepared by deposition at ambient temperatures on (100) MgO substrates. The NbTiN nanowires were fabricated from 2D films with thickness $d = 5$ nm by a conventional e-beam lithography method and a reactive ion etching method with CF_4 plasma. As a result, we observed negative current-voltage characteristics (n-IVC) as a function of magnetic field due to field induced superconductivity. One of reasons for n-IVC is based on the suppression of the non-equilibrium charge imbalance process at normal and superconducting boundaries, namely, at the boundaries between phase-slipped and superconducting regions in SNWs. Although the exact mechanism is unsolved, it is reasonable to consider that the one of the reason for n-IVC concerns with the existence of phase slip centers originating the behaviors of Thermal activation phase slip (TAPS) and/or quantum phase slip (QPS). In addition, we will argue observed the n-IVC is caused by entry of vortices in the nanowire. We also propose a concept of flux-based superconducting devices without using the nanowires.

Keywords: nanowire, phase slip